Solid Freeform Fabrication 2021: Proceedings of the 32nd Annual International Solid Freeform Fabrication Symposium – An Additive Manufacturing Conference
Reviewed Paper

Evaluation of Early Fatigue Damage Detection in Additively Manufactured AlSi10Mg

Susheel Dharmadhikari[1] and Amrita Basak[1, *]

[1]Department of Mechanical Engineering,
The Pennsylvania State University, University Park, PA 16802

* Corresponding Author: aub1526@psu.edu

Abstract

The article presents two distinct measures for fatigue damage detection in additively manufactured AlSi10Mg specimens with a one-sided V-notch. The specimens are fabricated on a ProX-320 laser powder bed fusion equipment with recycled AlSi10Mg powders using vetted process parameters as suggested by 3D Systems. The process of fatigue damage evolution is monitored using two heterogeneous sensing techniques, namely, the force-displacement sensors and a confocal microscope. The force and displacement sensors are embedded in the fatigue testing apparatus to capture the global effects of the stress-strain behavior of the specimens; however, it provides no information about the local damage near the notch. The force-displacement time-series data, which shows a hysteresis-like behavior, is calibrated using a confocal microscope focused inside the notch of the specimen so that the onset of fatigue crack initiation can be detected at a crack opening displacement (COD) of ~10 microns. Using the force-displacement data, the energy dissipation rate and the material stiffness per cycle are computed. The results show a detection accuracy of 96.25% and 90.84% for the energy dissipation rate and material stiffness per cycle, respectively. In conclusion, the paper establishes two successful predictors for fatigue damage detection in additively manufactured AlSi10Mg specimens.

Keywords
Fatigue Failure Detection; Laser Powder Bed Fusion; Force-Displacement Sensors; Confocal Microscope

1. Introduction

While over the past few decades, additive manufacturing (AM) has generated a tremendous amount of excitement within the materials and manufacturing community, sub-par mechanical properties (e.g., fatigue) continue to challenge the researchers across industry and academia [1]. A considerable volume of research exists with regards to *online real-time* fatigue damage detection for traditionally fabricated metallic materials via different sensing technologies such as ultrasonics [2], acoustic emissions [3], eddy currents [4], etc. The fundamental working principle of such sensing techniques are based on three cardinal pillars: (i) acquisition of the sensor data in the form of a time-series; (ii) classification (e.g., healthy and cracked) of the time-series data using a secondary sensor (frequently an imaging one such as a digital or an optical microscope); (iii) application of time-series pattern recognition techniques to pinpoint the damage solely based on time-series without any requirement of the secondary sensor as it would be unrealistic to have an imaging sensor when a component is operating in the field. The efficacy of the method sensors is acid-tested by their capability in detecting the length-scale of fatigue cracks [4] which consist of a

range of length scales starting from microns to millimeters [5]. The state-of-the-art on traditionally manufactured components shows successful damage detections when the crack opening displacement (COD) is in the millimeter scale length [6]. COD, as the name suggests, corresponds to the distance between the ends at the base of a crack. A representative notched region of the specimen with a schematic for COD (and crack length) is shown in Fig. 1(a) and (b). Traditionally, the research has been focused towards studying crack length but with recent studies [5], it has been shown that COD is an earlier indicator of crack emergence. Irrespective of whether the component is traditionally or additively fabricated, an important research direction in this area is, therefore, to enable the detection of fatigue damages in the micron-scale COD [5].

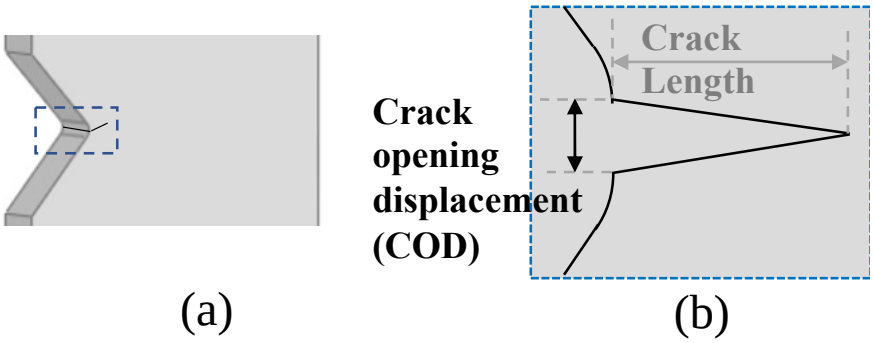

Figure 1: (a) An overview of the notched region of a specimen with a crack, (b) Schematic highlighting the crack opening displacement (COD)

To achieve this progression and that too for AM components, the research presented in this article develops a method for fatigue damage detection at the micron-scale COD using an energy dissipation approach [7, 9] where a high-precision confocal microscope is used for data calibration. Energy dissipation due to material hysteresis has been carried out with strain-controlled experiments for traditionally fabricated metallic specimens to date [7]. This article presents a complementary energy dissipation interpretation for *stress-controlled* experiments for AM specimens. The study characterizes the force and displacement time-series data during fatigue tests collected using an embedded load cell and a linear variable differential transformer (LVDT), respectively. Using the time-series data, an energy-dissipation-based metric and a stiffness metric are derived and their efficiencies in detecting fatigue damages in AM AlSi10Mg specimens are quantified.

2. Experimental

2.1. Materials and Specimen

Recycled AlSi10Mg powder obtained from 3D Systems is used in the present study. The composition of the powder as obtained via energy dispersive x-ray spectroscopy (EDS) is: 86.83 wt. % Al, 11.83 wt. % Si, 0.34 wt. % Mg, 0.96 wt. % O, and 0.04 wt. % Fe. ASTM E466 standard AlSi10Mg specimens as shown in Fig. 2(a) are used in this study. An actual picture of the specimen highlighting the build direction is shown in Fig. 2(b). From a static tensile simulation using SolidWorks, the stress concentration factor K_t is evaluated to be 5.45.

The specimens are fabricated on a ProX-320 (3D Systems, Rock Hill, South Carolina, USA) laser powder bed fusion (L-PBF) equipment housed at the Center for Innovative Materials Processing through Direct Digital Deposition (CIMP-3D) at Penn State using vetted process parameters suggested by 3D Systems. The parameters used for fabricating the specimens are as follows: layer thickness of 60 μm, laser power of 325 W, and scanning speed of 1400 mm/s. A striped hatch design pattern with hatch spacing 82 μm is used. The specimens used in the tests are in as-built condition without any post-processing.

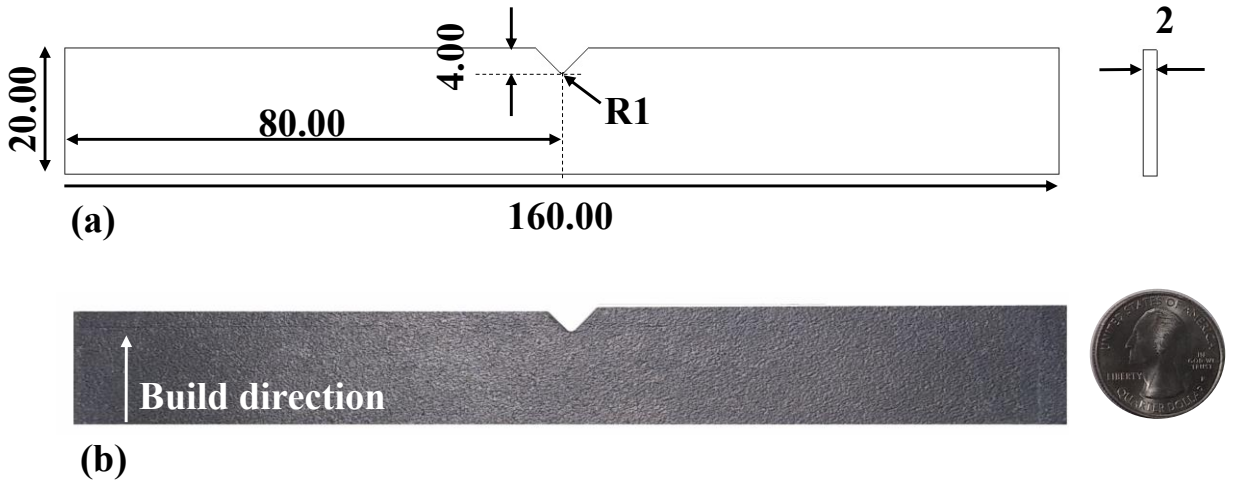

Figure 2: (a) Geometry of the one-sided V-notched specimen (dimensions in mm). (b) An image of the actual specimen with an American quarter for scale.

2.2. Fatigue Testing Apparatus

The fatigue experiments are performed on an MTS Elastomer 831.10 servo hydraulic setup (Fig. 3(a)) which is equipped with a high-precision confocal microscope. The fatigue test is configured to apply a sinusoidal uniaxial tensile loading with a maximum force of 3 kN and a stress ratio (min. force / max. force) of 0.33 at a frequency of 20 Hz resulting in a maximum nominal stress of 93.75 MPa and a stress amplitude of 31.2 MPa in the specimen. Based on the fatigue strength of AlSi10Mg, these loading conditions ensure a stress-dominated low-cycle fatigue failure in the specimens. The fatigue test is controlled through an automated routine from the Multi-Purpose TestWare^{TM} (MPT) software suite available for the MTS FlexTest$^{®}$ controller. The MTS system can measure the force (F) and displacement (D) responses in the form of a time-series during a test using an embedded load cell and LVDT, respectively. The F-D data, which is acquired through the MPT routine, is captured at 6144 Hz. To calibrate the F-D time-series data for pinpointing the onset of fatigue damage initiation, a high-precision confocal microscope (Bruker Alicona, Graz, Austria) is used. The microscope can detect fatigue damages with a COD of 3 μm. A recent study [5] shows that the microscope orientation shown in Fig. 3(b) can detect a fatigue crack earlier. Fig. 3(c) shows the image of the notch base before the testing. During the test, the MPT routine is programmed such that the periodical loads are stalled every 500 cycles.

This stall is maintained at the maximum load and the period during the stall is used to monitor the base of the notch using the confocal microscope. If a crack is observed during the monitoring, the imaging is performed.

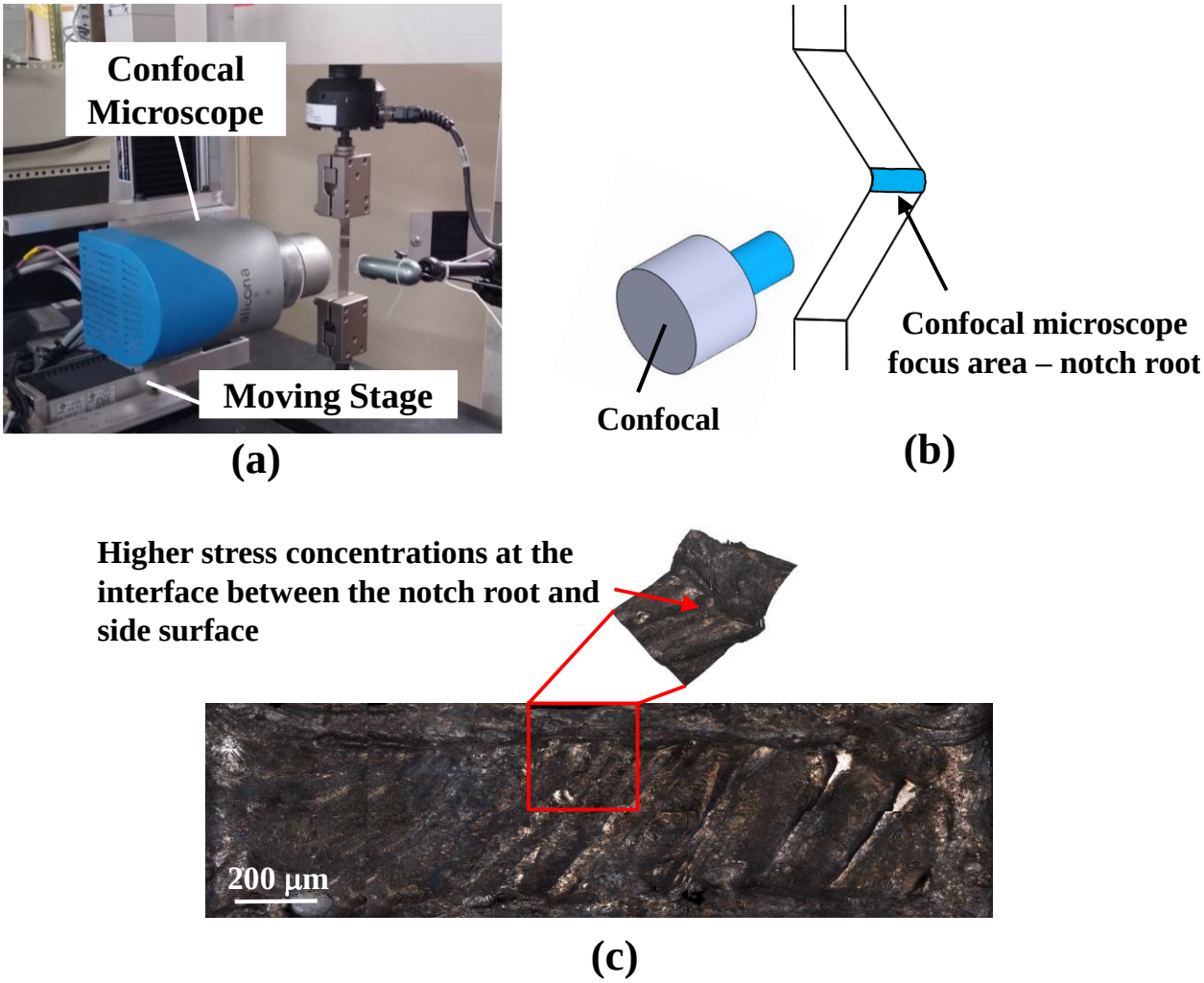

Figure 3. (a) Customized fatigue testing apparatus showing the specimen, the MTS testing system, the confocal microscope, and the moving stage. (b) A schematic illustrating the focus of the confocal microscope at the base of the notch. (c) Optical microscope image showing the entire base of the notch before fatigue testing.

3. Results and Discussion

3.1. Confocal Microscope-Based Imaging

A series of images taken during one of the fatigue tests are shown in Fig. 4. At the beginning of the test (Fig. 4(a), N = 0 cycles), the base of the notch does not indicate any damage. With the

progression of the fatigue damage, surface cracks start to emerge at about N = 8000 cycles (Fig. 4(c)). The surface crack then becomes a visible crack at N = 10500 (Fig. 4(d)) cycles and corresponds to a COD of 10 μm. A further growth in COD is observed with an increase in the number of load cycles.

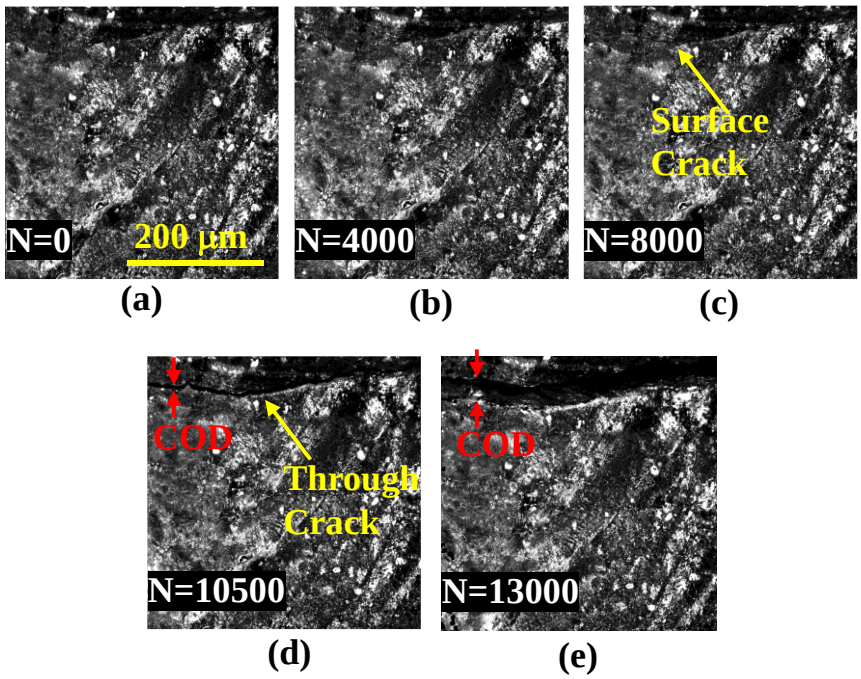

Figure 4: (a) to (e) - A chronology of the evolution of a fatigue crack captured through the confocal microscope for a representative AlSi10Mg specimen.

3.2. Force-Displacement Data

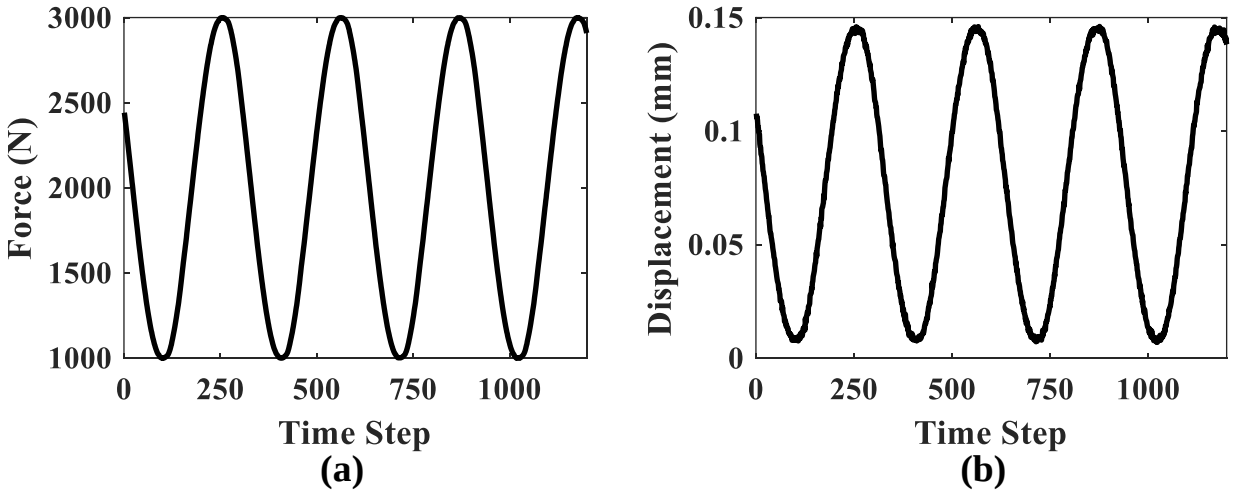

Figure 5: (a) Sinusoidal force (F) data for four cycles measured by the load cell. (b) Sinusoidal displacement (D) data for four cycles measured by LVDT.

Owing to the sinusoidal nature of the controlled loading experiments, the specimens exhibit a sinusoidal displacement response. Fig. 5(a) and 5(b) show the F-D time-series data for a representative (here, four) cycles measured through the load cell and LVDT, respectively. The F data shows a comparatively smoother operation due to the controlled application, however, the D data shows some noisy behavior around the peaks which can be attributed to measurement artifacts.

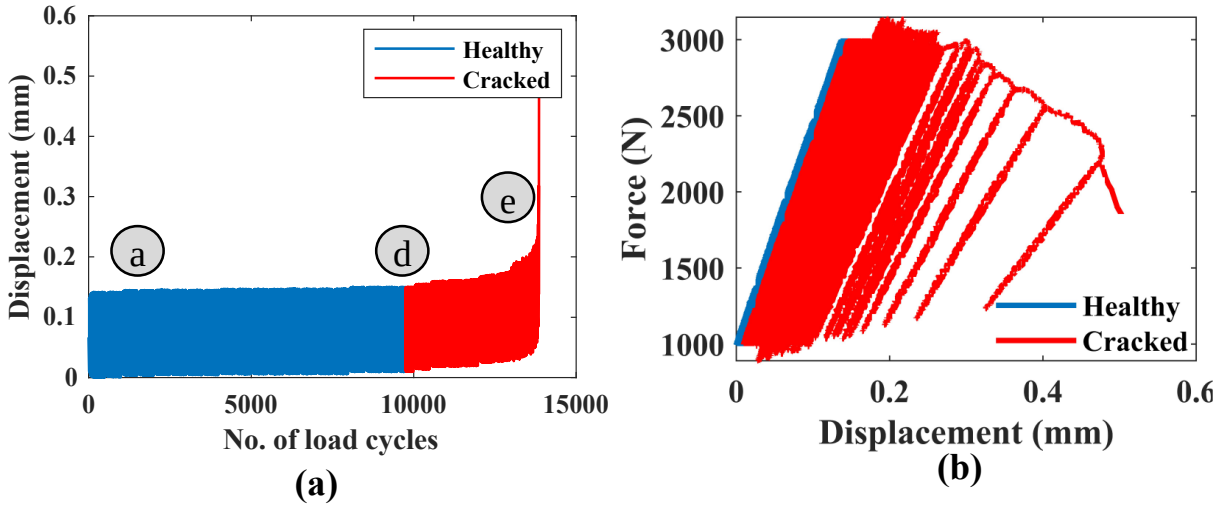

Figure 6: (a) D data during the entire fatigue test for a representative specimen with three indicators correlated with the microscope images in Fig. 4(a), (d), and (e). (b) Hysteresis behavior shown by the F-D time-series data.

The sinusoidal nature of the D data, however, is a local behavior as due to the damage accumulation, the D data of the specimen shows a gradual growth in its average magnitude as shown in Fig. 6(a) which is plotted against the number of time steps. Captured at 6144 Hz, the F-D time-series data is rich in the number of data points (i.e., timesteps) with roughly 300 of them per cycle. For example, if a specimen is having a fatigue life of 13000 cycles, the F vs. D curve will have 13000 × 300 = 3.9 million data points in it. The D data (Fig. 6(a)) is classified into healthy and cracked regions based on the synchronous information obtained from the confocal microscope. The gradual increase in the displacement is attributed to the increase in strain and subsequent crack growth in the specimen. The transition from the healthy region to the cracked region corresponds to the timestep where the confocal microscope measures a crack with COD 10 μm which is roughly in the short crack regime [5]. Fig. 6(b) shows the hysteresis-like nature by plotting the F-D time series data. The gradual increase in the area under the curve is attributed to the energy dissipated during the fatigue test. The curve is again classified into the healthy and cracked regions. The disparity between the energy dissipation before and after a crack develops is evident from Fig. 6(b).

3.3. Energy Dissipation Rate (EDR)

Motivated by the drastic difference in the distribution of the energy dissipation of the healthy and cracked regions as shown in Fig. 6(b), the rate of energy dissipation is hypothesized to contain

the information regarding the fatigue damage. Conventionally, the energy dissipated due to hysteresis is computed with the area under the curve during one cycle [7]. Since this approach is suitable for low cycle fatigue phenomena where the area under one cycle is significant, the approach is deemed to work for the present case as well. Fig. 7 illustrates the total change in displacement (ΔD, mm) and force (ΔF, N) during N cycles. Using these values, the energy dissipation rate (EDR) is defined as:

$$EDR = \frac{\Delta F \times \Delta D}{N}$$

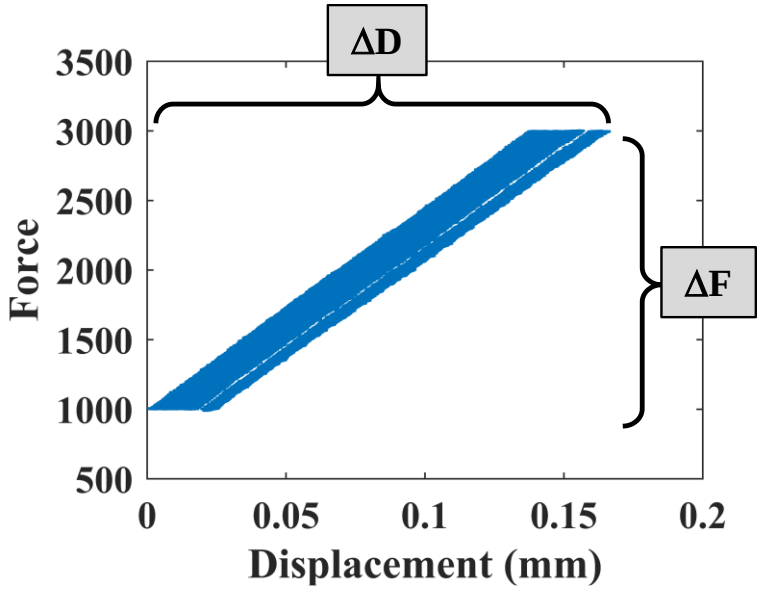

Figure 7: Hysteresis behavior for a representative N fatigue cycles showing the total change in force (ΔF) and displacement (ΔD).

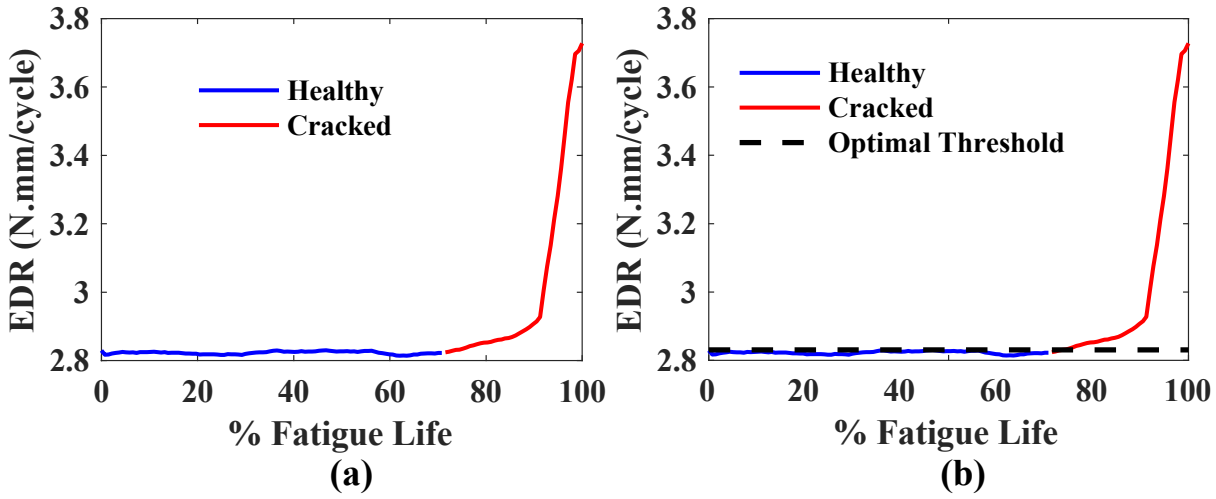

Figure 8: (a) EDR behavior with respect to the normalized fatigue life. (b) EDR curve with the optimal threshold computed using receiver operating characteristics (ROC).

Therefore, with this definition, EDR denotes the average loss of energy during N cycles. In this study, N is maintained at 100 indicating that EDR is computed at every 100 cycles. The behavior of EDR during the entire fatigue test is shown in Fig. 8(a). For example, if a specimen has a fatigue life of 13000 cycles, the EDR curve will have 13000/100 = 130 data points in it. Such a volume of data is sufficient for any pattern recognition techniques as reported in the open literature. As shown in Fig. 8(a), the specimen exhibits an EDR of around 2.82 N.mm/cycle at the beginning of the test. Each data point on the curve corresponds to the average energy lost during the 100 preceding cycles. The fatigue crack (with COD of 10 μm) detection through the confocal microscope is achieved at 0.7 of the normalized fatigue life. Shortly after the detection, the EDR tends to show a steady growth which is exponential near the end of the life where a fracture is imminent.

Table 1: Confusion matrix for EDR.

EDR	Predicted Healthy	Predicted Cracked
Truly Healthy	100%	0%
Truly Cracked	7.5%	92.5%

Such a sensitivity of EDR to the damage detection presents an excellent tool towards fatigue damage detection. Combining this information from EDR curve and machine learning, a classifier is built using an optimal thresholding-based technique using the receiver operating characteristics (ROC) to differentiate between a healthy and a cracked specimen [8]. The ROC computation provides an optimal threshold which acts as the boundary between a healthy state and a cracked state. During the fatigue test, if the EDR values are below this optimal threshold, then it can be inferred that the specimen is healthy. If the test indicates that the EDR is higher than the threshold, then the specimen can be assumed to be cracked. Fig. 8(b) plots the optimal threshold along with a representative EDR curve. The location where the EDR curve crosses the threshold corresponds to the damage detection. A mean threshold of 2.831 is observed for the EDR curve indicating the robustness of the metric. The accuracy of the classification from the workflow is tabulated through a confusion matrix [8] shown in Table 1. This confusion matrix shows the classifier can identify the healthy and cracked specimens with an accuracy of 100% and 92.5%, respectively.

3.4.Material Stiffness

In addition to that, the slope of the F-D time-series data is an important feature as illustrated from Fig. 6(b). The slope at the end of the red region is smaller than the slope at the beginning of the test. This slope corresponds to the material stiffness and the drop in it is attributed to material softening with the increase in fatigue damage [6]. From an energy perspective, the stiffness is an indicator of energy storage in the material. If F and D denote the total force and total displacement during one cycle, respectively, the stiffness during that cycle is represented as:

$$Stiffness = \frac{F}{D} \times \frac{160}{32} \times \frac{1}{1000}$$

The numerical multipliers 160 and 32 represent the length and area of the cross-section and are used to convert the stiffness into GPa. The above computation is performed for every cycle and the result is shown in Fig. 9(a).

The drastic drop in the material stiffness after the damage detection via the confocal microscope can be clearly observed. Like EDR, the damage detection rules are established for the stiffness curve. Fig. 9(b) shows the optimal threshold for a representative stiffness curve. The threshold shows a value of 71.57 GPa. Using the stiffness curves, an accuracy of 82.54% is observed in detecting the cracked specimens as opposed to 99.14% in detecting healthy specimens as shown in Table 2.

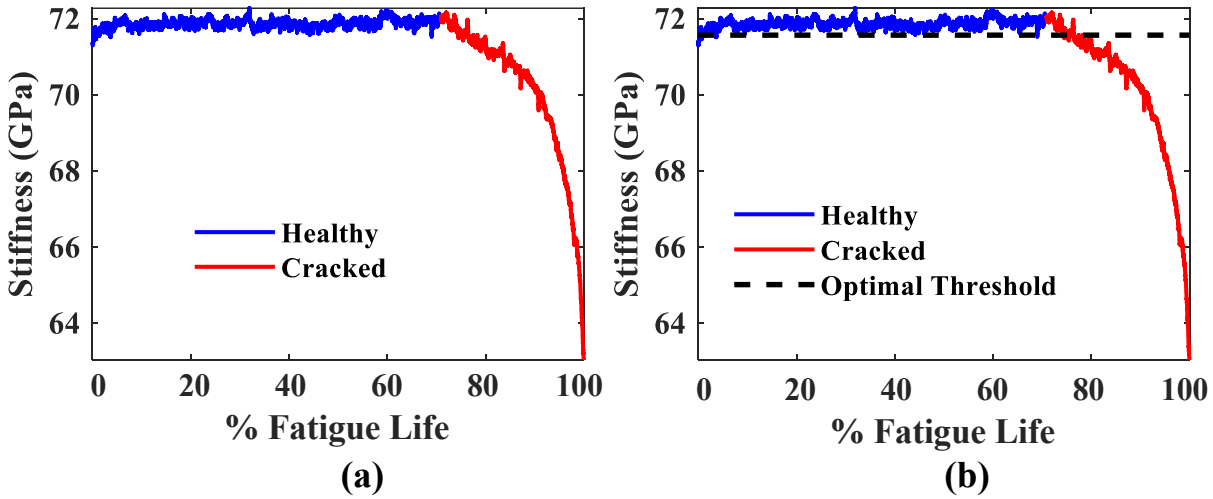

Figure 9: (a) Stiffness behavior with respect to the normalized fatigue life. (b) Stiffness curve with the optimal threshold computed using ROC.

Table 2: Confusion matrix for stiffness.

Stiffness	Predicted Healthy	Predicted Cracked
Truly Healthy	99.14%	0.86%
Truly Cracked	17.46%	82.54%

4. Conclusion and Future Work

The article presents two distinct metrics to assess fatigue damage detection in AM AlSi10Mg alloys. EDR and material stiffness show an accuracy of 96.25% and 90.84%, respectively for

detecting a crack with a COD of 10 μm. It is to be noted that the metrics presented in this study are specific to the loading conditions used in this study. A more detailed parametric analysis exploring the dependence of these metrics on loading conditions can expand the application of the proposed analysis to more general scenarios. Moreover, the distribution of the metrics for large number of specimens can also shed light on the consistency of the manufacturing process. In the future, the current work will be extended to study the behaviors over larger number of specimens with the effects of various build directions, specimen geometries, and AM process parameters [9].

5. Acknowledgments

The research reported in this paper is supported in part by the Department of Mechanical Engineering at the Pennsylvania State University, University Park, PA 16802. Any opinions, findings, and conclusions in this paper are those of the authors and do not necessarily reflect the views of the supporting institution.

6. References

[1] A. Yadollahi and N. Shamsaei, "Additive manufacturing of fatigue resistant materials: Challenges and opportunities," *International Journal of Fatigue,* vol. 98, pp. 14-31, 2017.

[2] S. Gupta, A. Ray, and E. Keller, "Online fatigue damage monitoring by ultrasonic measurements: A symbolic dynamics approach," *International Journal of Fatigue,* vol. 29, no. 6, pp. 1100-1114, 2007.

[3] N. Eleftheroglou and T. Loutas, "Fatigue damage diagnostics and prognostics of composites utilizing structural health monitoring data and stochastic processes," *Structural Health Monitoring,* vol. 15, no. 4, pp. 473-488, 2016.

[4] J. M. Papazian *et al.*, "Sensors for monitoring early stage fatigue cracking," *International Journal of Fatigue,* vol. 29, no. 9-11, pp. 1668-1680, 2007.

[5] S. Dharmadhikari, E. Keller, A. Ray, and A. Basak, "A dual-imaging framework for multi-scale measurements of fatigue crack evolution in metallic materials," *International Journal of Fatigue,* vol. 142, p. 105922, 2021.

[6] E. Keller and A. Ray, "Real-time health monitoring of mechanical structures," *Structural Health Monitoring,* vol. 2, no. 3, pp. 191-203, 2003.

[7] R. I. Stephens, A. Fatemi, R. R. Stephens, and H. O. Fuchs, *Metal Fatigue in Engineering*. John Wiley & Sons, 2000.

[8] C. M. Bishop, *Pattern recognition and machine learning*. Springer, 2006.

[9] S. Dharmadhikari and A. Basak, "Energy dissipation metrics for fatigue damage detection in the short crack regime for aluminum alloys," *Proceedings of ASME Turbo Expo 2021: Turbomachinery Technical Conference and Exposition* (pp. GT2021-58787). The American Society of Mechanical Engineers (ASME).